*Int. J. Multiphase Flow* Vol. 19, No. 5, pp. 875–886, 1993
Printed in Great Britain. 

0301-9322/93 $6.00 + 0.00


# SEDIMENTATION OF SOLID PARTICLES IN OIL-IN-WATER EMULSIONS

Y. YAN† and J. H. MASLIYAH‡
Departament of Chemical Engineering, University of Alberta, Edmonton, Alberta, Canada T6G 2G6

*(Received 13 November 1991; in revised form 25 May 1993)*

**Abstract**—This study reports experimental results on the sedimentation of spherical glass beads in oil-in-water emulsions. The oil droplets had a volume/surface mean diameter of about 10 $\mu$m. Three different sizes of glass beads were used, namely, 29, 57 and 157 $\mu$m. The solids volume fraction, based on the total volume, was varied up to 0.4; and the oil volume concentration, solids free basis, was varied up to 40%. The fingering phenomenon was observed for the case of the small solids of 29 $\mu$m. As a result, both the settling velocity of the solids and the creaming velocity of the oil droplets were significantly enhanced. For the case of the intermediate solids (57 $\mu$m), no fingering was observed when the solids settled in a 20% oil emulsion. The settling velocity of the solids can be predicted by assuming the emulsion to form a continuous phase. However, fingering was observed when the solids settled in a more concentrated (40%) emulsion. For the case of the large solids (157 $\mu$m), no structure of any kind was observed. The solids settling velocity can be predicted by assuming the emulsions to form a continuous phase. For the low oil concentration (20%) emulsion system, the conditions for the onset of internal structures (fingering) for the different solids were consistent with previous experimental observations for the case of bidisperse solids suspensions.

*Key Words:* bidisperse sedimentation, oil-in-water emulsion, fingering phenomena

## INTRODUCTION

Gravity separation of bidisperse suspensions is an important industrial process, and there exists a large amount of literature on this subject. For dilute systems, the particles of different species can be uniformly distributed throughout the suspension, and the settling behaviour of a bidisperse system can be well-described by models proposed by Lockett & Al-Habbooby (1974), Mirza & Richardson (1979), Masliyah (1979), Selim *et al.* (1983) and Patwardhan & Tien (1985). However, for certain bidisperse systems, when the solids volume fraction exceeds a certain value, a uniform lateral distribution of the light and the heavy particles in the suspension cannot be maintained. The heavy particles tend to laterally gather together and settle in small vertical columns, which gives rise to the *fingering phenomenon.* As a result, the apparent settling velocity of the heavy particles and the rising velocity of the light particles are both increased. The fingering phenomenon was first reported by Whitmore (1955) and was investigated extensively by Weiland and his co-workers (Weiland & McPherson 1979; Fessas & Weiland 1981, 1982, 1984; Weiland *et al.* 1984). MacTaggart *et al.* (1988) studied settling in an inclined container with the fingering phenomenon being present.

Batchelor & Janse van Rensburg (1986) developed a theoretical criterion to predict the onset of fingering. It was concluded by the authors that the inhomogeneities are not necessarily fingering-like. In a broader sense, the authors referred to the inhomogeneities as *internal structures.* They attributed the formation of internal structures to the instability of the statistically homogeneous dispersion to a small concentration disturbance for a certain combination of the size ratio and the density ratio of the two types of particles and their volume fractions. The instability theory was consistent with their own experimental observations and also with those of Fessas & Weiland (1984) and Weiland *et al.* (1984).

†Present address: DuPont Canada Inc., Research Centre, P.O. Box 5000, Kingston, Ontario, Canada K7L 5A5.
‡To whom all correspondence should be addressed.

In the present study, we investigate the settling behaviour of a bidisperse system containing solid particles and small oil droplets. No previous studies have been conducted for this type of a system. The present study is a consequence of our earlier investigation on the rheology of oil-in-water emulsions with added solids. The rheological studies of Yan *et al.* (1991) and Yan & Masliyah (1993) indicated that for oil having viscosities comparable to water, the oil-in-water emulsions behaved as a continuous phase when the solids were 3 times larger than the oil droplets. However, for very viscous oils, the emulsions behaved as a continuous phase when the solids were about 10 times larger than the oil droplets.

## EXPERIMENTAL

### *Materials*

The oil used was a refined mineral oil (Bayol-35), having a density of 780 kg/m$^3$ and a viscosity of 2.4 mPa s at 25°C. Triton X-100, a non-ionic water soluble emulsifier was used to stabilize the oil-in-water emulsions. The solid particles used were spherical glass beads having a red colour with a density of 2530 kg/m$^3$. The supplied glass beads were screened through standard sieves in a sieve shaker to give narrow size distribution fractions. The volume/surface mean diameters of the three size fractions used in the present study were 29, 57 and 157 $\mu$m.

### *Procedure*

The emulsions were first prepared in batches of approx. 1 liter. The oil was slowly added to a 1% Triton X-100 water solution under the action of shear using a Gifford-Wood (model 1-LV) homogenizer. The oil-and-water mixture was then continuously sheared for 10 min after the oil addition. The oil droplets in the emulsion had a volume/surface mean diameter of about 10 $\mu$m. The cumulative size distribution of the oil droplets is shown in table 1. The viscosity of the emulsion was measured using a coaxial cylinder viscometer (Contraves Rheomat 115). The viscosity of the 20 and 40% emulsions were 2.0 and 4.8 mPa s, respectively. Both emulsions showed Newtonian behaviour and were very stable.

Batch sedimentation experiments were conducted at room temperature in a vertical rectangular plexiglas container having internal dimensions of 40 × 8.2 × 1.7 cm. The vertical alignment of the settler was ensured by adjusting the three screw nuts located on its base using a spirit level before each run.

Solid particles were first soaked in the 1% Triton X-100 water solution. The water was then filtered out and the *water-wet* solids were then added to the already prepared emulsion in the settler. For a given amount of emulsion (at certain oil concentration) in the settler, solids were added in different batches over a wide range of volume fraction.

The mixing of solids and emulsion was provided by moving a small piece of T-shape wooden stirrer manually up and down in the settler. Care was also taken to allow any small bubbles to escape after solids were added to the emulsion prior to any measurements. In the present study, the oil volume concentration ($\beta$) was calculated based on the volume of oil and water only, whereas the solids volume fraction ($\varphi_S$) was calculated based on the total system volume, i.e. water + oil + solids. The oil volume fraction based on the total volume is then $\beta(1 - \varphi_S)$.

Due to the distinct colours of the red glass beads and the "white" emulsion, it was possible to track the solids settling upper interface throughout the sedimentation process at solids volume fractions above 0.1. Below this volume fraction, a distinct interface could be observed only at the initial settling stage. The interface became less clear as settling proceeded. In general, the bottom rising interface of the solids sediment, referred to as the lower interface, could also be tracked. The main interest of this study is confined to the solids upper settling interface within the emulsion phase.

Table 1. Cumulative size distribution of the oil droplets

| $d$ ($\mu$m) | 2.5 | 6.5 | 9.5 | 16.5 |
|---|---|---|---|---|
| % Undersize | 53.4 | 76.1 | 86.7 | 100 |

## RESULTS AND DISCUSSION

### *Visual observations*

Experiments were first performed on emulsion creaming prior to any solids addition. The rising interface between the "white" emulsion and the clear water is very sharp and can thus be tracked very accurately. However, the interface between the "sediment" at the top and the ongoing creaming emulsion was difficult to observe, although such a layer of concentrated emulsion is present on the top.

Figures 1(a) and (b) show the sedimentation process of the small size beads (29 $\mu$m) in a 20% emulsion. The solids volume fraction was 0.30. Both creaming and fingering were observed during the settling. The formation of visible streams took some time to set up (up to 30 s), and the diameter of the established streams was in the range of a few millimetres. Comparison between figures 1(a) and (b) indicates that the streams become finer as settling proceeds. The streams disappear completely shortly before the disengagement between the emulsion and the settling solids. After disengagement, the solids continue to settle in pure water with the emulsion creaming above. For this solids size, the fingering streams were observed at solids volume fractions $>0.1$. A similar description of fingering phenomenon was also given by Fessas & Weiland (1984). The photographs from the present study show a more regular streams pattern than those given by Batchelor & Janse van Rensburg (1986). The aforementioned studies dealt with bidisperse solids suspension.

For the case of the intermediate solid size (57 $\mu$m) settling in a 20% oil emulsion, the solids appeared to be uniformly distributed in the emulsion throughout the whole settling period. However, strong fingering was observed when the solids settled in the more concentrated (40%) emulsion. The fingering structure was similar to that shown in figures 1(a) and (b).

For the case of the large solids size (157 $\mu$m), the solids were uniformly distributed throughout the emulsion for both the 20 and 40% emulsions, and no fingering was observed.

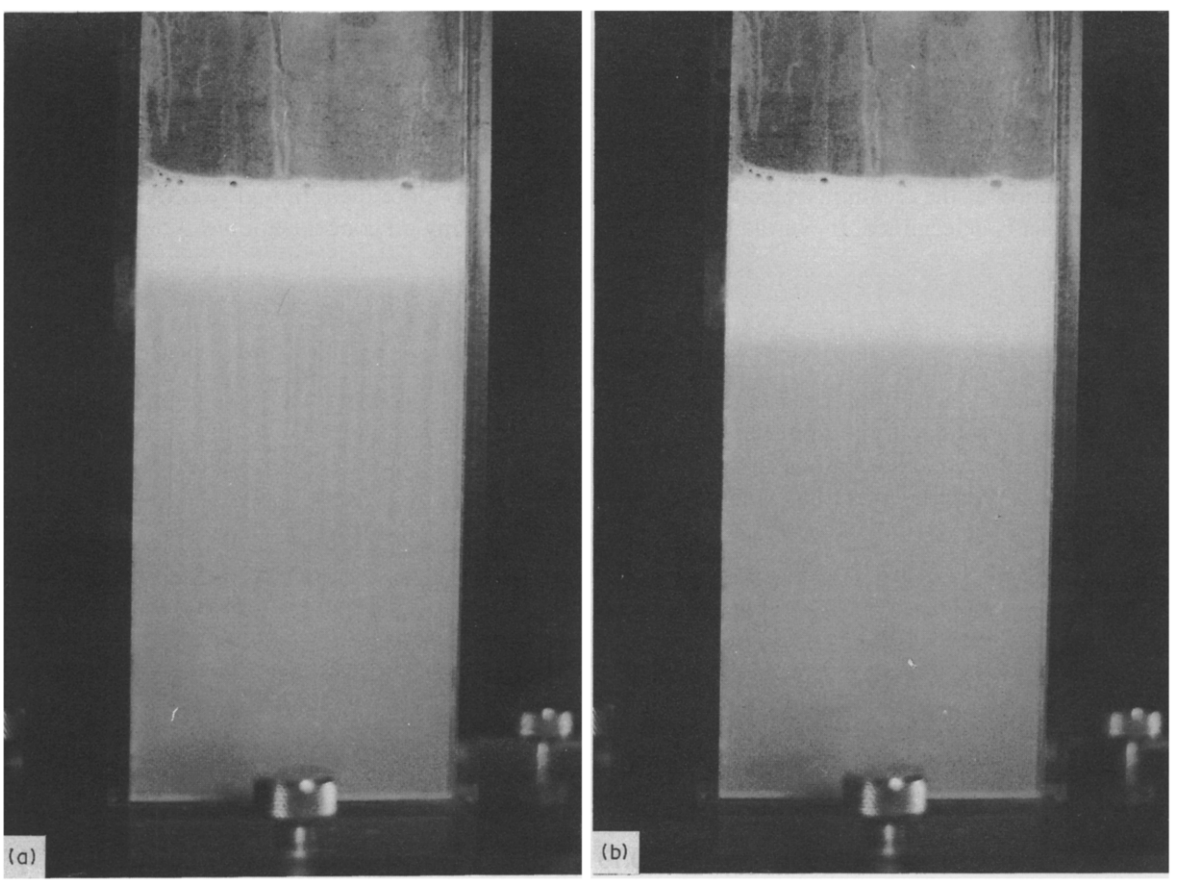


Figure 1. Settling process of the small size solids (29 $\mu$m) in a 20% emulsion with $\varphi_S = 0.30$: (a) $t = 180$ s, strong fingering; (b) $t = 283$ s, weak fingering.

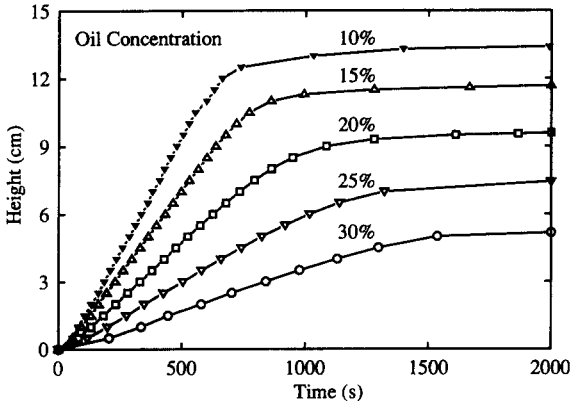


Figure 2. Variation of the emulsion creaming interface height with time for different oil emulsion concentrations.

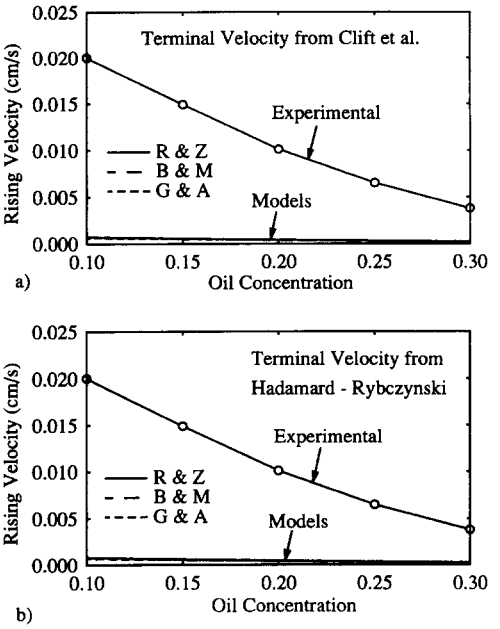


Figure 3. Comparison of the emulsion creaming velocity between the experimental and the predicted values.

*Emulsion creaming*

Figure 2 shows the variation of the creaming emulsion interface height with time for emulsions having different oil concentrations. The initial part of the creaming curve is linear except for one or two data points near the origin. Towards the end of the creaming process, the emulsion interface rise velocity decreased with time. The creaming velocity was determined from the slope of the linear part of height versus time curves. As would be expected, the creaming velocity decreased with increasing oil concentration.

Prediction of the creaming velocity can be made as follows. Once the terminal velocity of a single oil droplet is determined, the hindered creaming velocity at any oil concentration can be calculated from

$$U_\varepsilon = U_t F(\varepsilon) = U_t F(1-\varphi), \qquad [1]$$

where $\varepsilon$ is the porosity of a suspension or an emulsion, i.e. the continuous phase volume fraction and $\varphi$ is the volume fraction of the dispersed phase; $U_t$ is the terminal velocity of a single particle settling in the same continuum and the same container, i.e. the wall effect is taken into account; and $F(\varepsilon)$ is a hindered settling function.

The terminal velocity of a single particle settling in an infinite fluid, $U_{t\infty}$, can be determined from Clift *et al.* (1978):

$$U_{t\infty} = \frac{gd^2(\rho_p - \rho_f)}{18\mu_f} G(\mathrm{Re}_{t\infty}), \qquad [2]$$

where $\mathrm{Re}_{t\infty} = (\rho_f U_{t\infty} d/\mu_f)$, $d$ is the diameter of the oil droplet and $\rho_p$ is the density of the oil; $\rho_f$ and $\mu_f$ are the density and viscosity of the continuous (water) phase, respectively. $G(\mathrm{Re}_{t\infty})$ can be evaluated from

$$G(\mathrm{Re}_{t\infty}) = (1 + 0.1315\mathrm{Re}_{t\infty}^{(0.82 - 0.05\log_{10}\mathrm{Re}_{t\infty})})^{-1} \qquad [3]$$

for $\mathrm{Re}_{t\infty} < 200$.

Table 2. Some functional forms of $F(\epsilon)$

**Richardson & Zaki (1954):**

$$F(\varepsilon) = \varepsilon^n,$$

where

| | |
|---|---|
| $n = 4.65 + 19.5(d_p/w)$, | $Re_{t\infty} < 0.2$ |
| $n = 4.35 + 17.5(d_p/w)Re_{t\infty}^{-0.03}$, | $0.2 < Re_{t\infty} < 1$ |
| $n = (4.45 + 18.0(d_p/w)Re_{t\infty}^{-0.1}$, | $1 < Re_{t\infty} < 200$ |
| $n = 4.45Re_{t\infty}^{-0.1}$, | $200 < Re_{t\infty} < 500$ |
| $n = 2.39$, | $Re_{t\infty} > 500$. |

**Barnea & Mizrahi (1973):**

$$F(\varepsilon) = \frac{\varepsilon^2}{1 + (1-\varepsilon)^{1/3} \exp\left[\frac{5(1-\varepsilon)}{3\varepsilon}\right]}, \quad \text{all } Re_t.$$

**Garside & Al-Dibouni (1977):**

$$F(\varepsilon) = \varepsilon^n,$$

where

$$\frac{5.1 - n}{n - 2.7} = 0.1Re_t^{0.9}, \quad \text{all } Re_t.$$

$U_t$ and $U_{t\infty}$ are related by the following expression (Francis 1933):

$$U_t = U_{t\infty}\left[\frac{1 - 0.475\left(\frac{d}{w}\right)}{1 - \left(\frac{d}{w}\right)}\right]^{-4} \qquad [4]$$

for $Re_t < 0.2$, where $Re_t = \rho_f U_t d/\mu_f$ and $d/w$ is the ratio of the particle diameter to the containers smallest dimension. For $0.1 < Re_t < 1000$, Garside & Al-Dibouni (1977) suggested the following relationship:

$$U_t = U_{t\infty}\left[1 + 2.35\left(\frac{d}{w}\right)\right]^{-1}. \qquad [5]$$

The most commonly used functional forms of $F(\varepsilon)$ are those of Richardson & Zaki (1954), Barnea & Mizrahi (1973) and Garside & Al-Dibouni (1977). They are listed in table 2.

Figure 3(a) shows the calculated creaming velocity using [1] and the above-mentioned three functional forms for $F(\varepsilon)$. The terminal velocity of a single oil droplet was determined from [2]. As can be seen, the three models yielded little difference and the calculated creaming velocity is much lower than the experimental values.

Figure 3(b) shows similar plots to those in figure 3(a) except that the terminal velocity is calculated from the Hadamard–Rybczynski formula for a liquid droplet (Clift *et al.* 1978):

$$U_{t\infty} = \tfrac{2}{3}g\left(\frac{d}{2}\right)^2 \frac{\Delta\rho}{\mu_f}\left(\frac{1+k}{2+3k}\right), \qquad [6]$$

where $k$ is the viscosity ratio of the dispersed phase to the continuous phase and $\Delta\rho$ is the density difference between the dispersed and the continuous phases. Again, the calculated creaming velocity is significantly lower than the experimental values. These results are surprising as one would expect that with possible electroviscous effects, the prediction would give a higher rising velocity than those measured experimentally. However, the opposite is observed in this study.

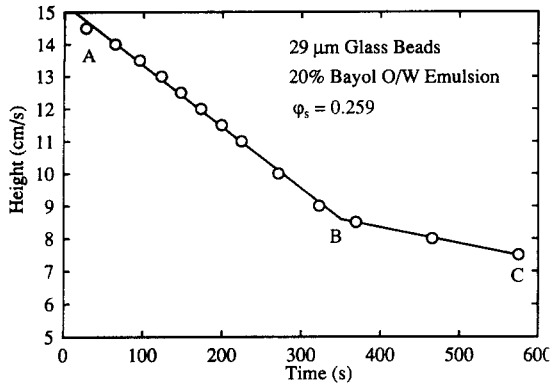


Figure 4. Variation of the solids settling interface height with time for the 29 $\mu$m solids and 20% emulsion.

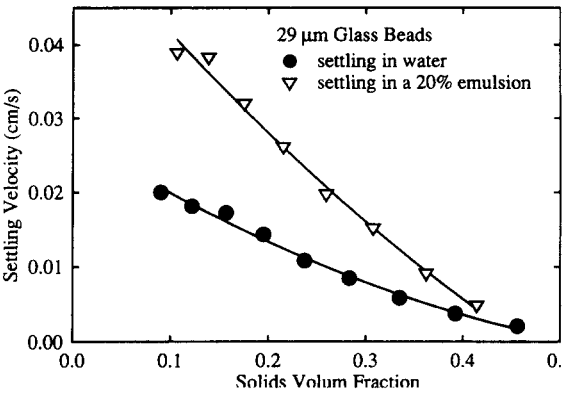


Figure 5. Solids settling velocities in water and in a 20% oil emulsion for the 29 $\mu$m solids.

*Settling of the small solids size (29 μm)*

A typical height vs time curve is shown in figure 4 for the (29 $\mu$m) glass beads at $\varphi_S = 0.259$ settling in a 20% oil emulsion. The data points follow two straight lines. For this system, the fingering phenomenon is present. The deviation of the first point from the linear relationship of height vs time is indicative of the fact that the fingering structure (streams) took some time to set up. This is also confirmed from visual observations. The first linear part (line AB) is for the settling of solids within the emulsion, and the second linear part (line BC) is for the settling of solids in pure water. The intersection of the two straight lines (point B) corresponds to the complete disengagement of the solids suspension and the emulsion. The slope of the straight lines represents the settling velocity of the solids. As can be observed, the slope of line AB is much higher than that of line BC. This indicates that the settling velocity of the solids in the emulsion is much higher than in water. This is attributed in part to the enhancement in settling due to the fingering phenomenon and to a higher solids concentration in the water zone.

Figure 5 compares the settling velocity of the (29 $\mu$m) glass beads settling in water and in a 20% emulsion over a wide range of solids volume fraction. The settling velocity of the solids in the 20% emulsion is significantly enhanced due to the presence of the oil droplets, typically by a factor of 2. Since the 20% emulsion has a viscosity of about 2 mPa s and nearly the same density as water, normal hindered settling should result in a reduced settling rate (also by a factor of 2). However, due to the presence of the light particles (oil droplets) and, in turn, the fingering phenomenon, the settling velocity is increased by a factor of 2 rather than reduced by a factor of 2.

The effect of oil concentration on the settling velocity of the solids in the emulsion is shown in figure 6 for four different solids volume fractions. At a given solids volume fraction, the solids settling velocity increases with increasing oil concentration and reaches a maximum at about 20%

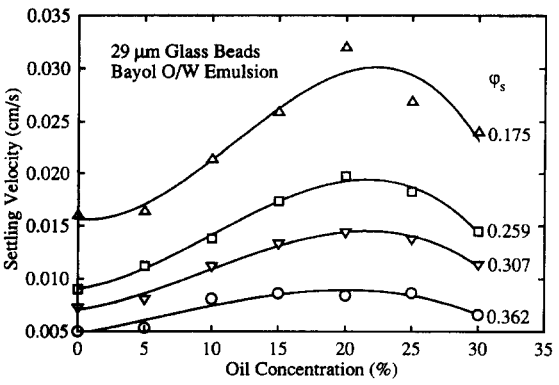


Figure 6. Effect of oil concentration on the solids settling velocity for the 29 $\mu$m solids.

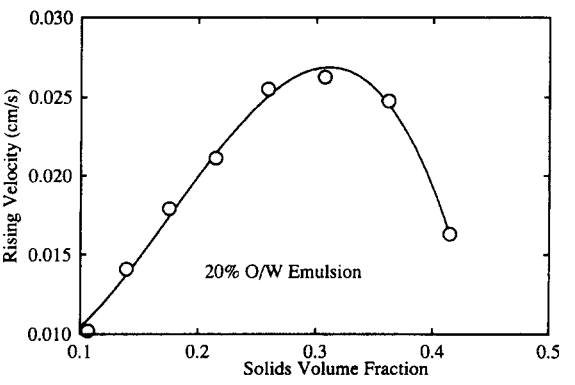


Figure 7. Effect of solids volume fraction on emulsion creaming velocity for the 29 $\mu$m solids.

oil concentration. Further increase in the oil concentration results in a decrease in the solid settling velocity.

The creaming velocity of emulsion was also enhanced due to fingering. Since it was difficult to follow the creaming interface in the presence of the fingering streams, the creaming velocity was calculated in a manner similar to the approach adopted by Fessas & Weiland (1984). The creaming velocity was calculated by measuring the time taken for the solids suspension and the emulsion to disengage from each other, and the position of the disengagement relative to the bottom of the settler. Figure 7 shows the variation of the creaming velocity with solids volume fraction for a 20% oil emulsion. As can be seen, the creaming velocity increases with solids volume fraction and reaches a maximum at a solids volume fraction of about 0.3.

A generalized correlation for predicting the enhanced settling velocity with fingering was developed by Fessas & Weiland (1984) for bidispersed solids suspensions. By making use of force balance between the gravity driving force in a stream and the viscous force exerted on the moving stream by the continuum, they were able to derive the following correlation:

$$\frac{4U_{rel}\mu_f\mu_{rb}}{(d_s+d_c)\Delta\rho_s^{\infty}g} = k'D\frac{\Delta\rho_s}{\Delta\rho_s^{\infty}}, \qquad [7]$$

where $U_{rel}$ is the relative velocity between the stream and the continuum, $\mu_f$ is the viscosity of the fluid, $\mu_{rb}$ is the relative viscosity with respect to the viscosity of the fluid and $d_s$ and $d_c$ are the paraticle diameters in the stream and in the continuum, respectively. In the present case, $d_s$ and $d_c$ are the diameters of the solids and the oil droplets, respectively. $D$ is the stream diameter, $k'D$ may be treated as an unknown parameter, $\Delta\rho_s$ is the density difference between the stream and the continuum and $\Delta\rho_s^{\infty}$ is the maximum (packed) density difference. Further details on evaluating $U_{rel}$, $\mu_{rb}$, and $\Delta\rho_s$ can be found in the original work of Fessas & Weiland (1984).

For the case where the fingering phenomenon is present, [7] can be used to compare the settling velocity of the solids in an emulsion system and in a bidisperse solids suspension. The data from the present study together with representative data for bidisperse solids suspension, taken from Fessas & Weiland (1984), are shown in figure 8. Although the settling data for both systems show similar trends, Fessas & Weiland's correlations for bidisperse solids systems do not accurately predict the settling data in an emulsion system.

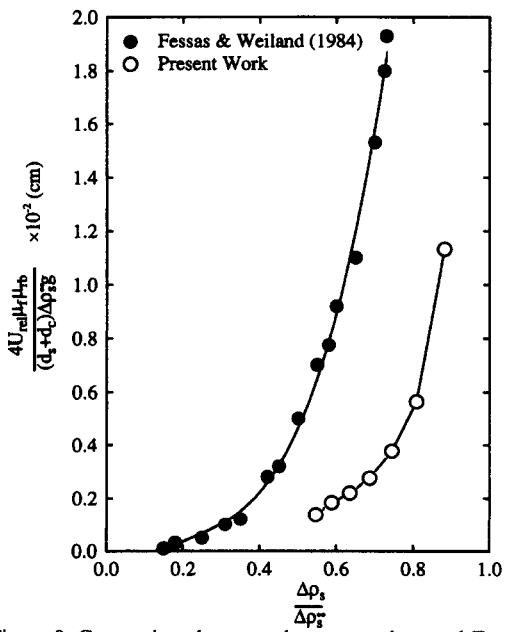


Figure 8. Comparison between the present data and Fessas & Weiland's (1984) data for bidisperse solids suspensions.

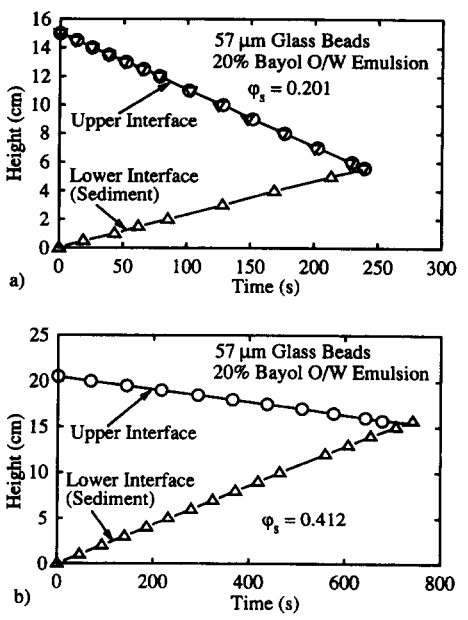


Figure 9. Variation of the solids settling interface and sediment rising interface with time for the 57 $\mu$m solids: (a) $\varphi_S = 0.201$; (b) $\varphi_S = 0.412$.

*Settling of (57 and 157 μm) size solids*

No fingering was observed when the 57 μm solids settled in a 20% oil emulsion. Figures 9(a) and (b) show the variation of the upper and lower solids interfaces with time for solids volume fractions of 0.201 and 0.412, respectively. The interfaces were followed till settling was complete. As can be seen, a linear relationship is observed between an interface height and time.

The settling velocity of solids in a continuum can be predicted using [1] together with the functional form of $F(\varepsilon)$ given in table 2. Equation [1] can be written as

$$\frac{U_\varepsilon}{U_t} = F(\varepsilon) = \varepsilon^n \qquad [8a]$$

and

$$\left(\frac{U_\varepsilon}{U_t}\right)^{1/n} = \varepsilon = 1 - \varphi_S. \qquad [8b]$$

Equations [8a, b] indicate that the measured settling velocity in a continuum, normalized by the terminal velocity of a single particle in that continuum, is a function of the solids volume fraction only and is independent of the continuum properties (density, viscosity). In this regard, [8] is useful in correlating the data for the 57 μm glass beads settling in water and in the 20% oil emulsions where the fingering phenomenon is absent. Figure 10 shows such plots as suggested by [8] using both the Richardson & Zaki [figure 10(a)] and the Garside & Al-Dibouni [figure 10(b)] correlations. As can be seen, the data for water and the 20% emulsion collapse together and can be well-represented by the models. Thus, the 20% emulsion can be regarded as a continuous phase towards the settling solids.

The fingering phenomenon was observed when the 57 μm size solids settled in the 40% emulsion. The experimental data for the velocity ratio, $U_\varepsilon/U_t$, for the case of the 40% emulsion is also shown in figure 10. The experimental data for the 40% emulsion lie well above those for water and 20% emulsion. This is attributed to the settling enhancement due to the presence of the fingering phenomenon.

For the case of 157 μm size solids, the fingering phenomenon was absent for both the 20 and 40% emulsions. Figure 11 shows plots of $(U_\varepsilon/U_t)$ vs solids volume fraction for water and 20 and 40% emulsions. As the fingering phenomenon was absent in both emulsions, the data for $U_\varepsilon/U_t$ collapsed together for the three fluids. Once again, such a collapse in the data indicates that the

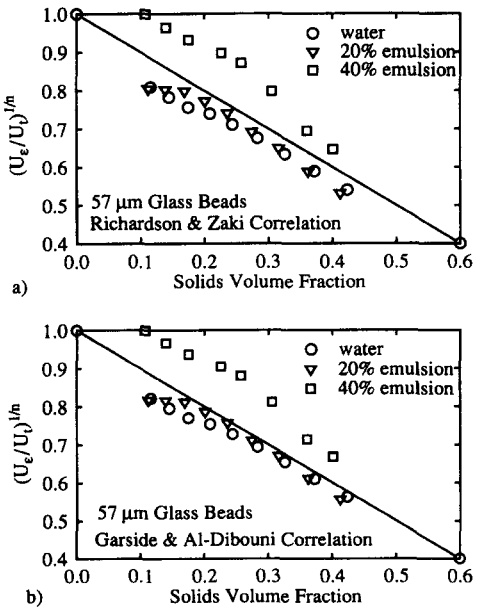


Figure 10. Solids settling data in water and in emulsions for the 57 μm glass beads.

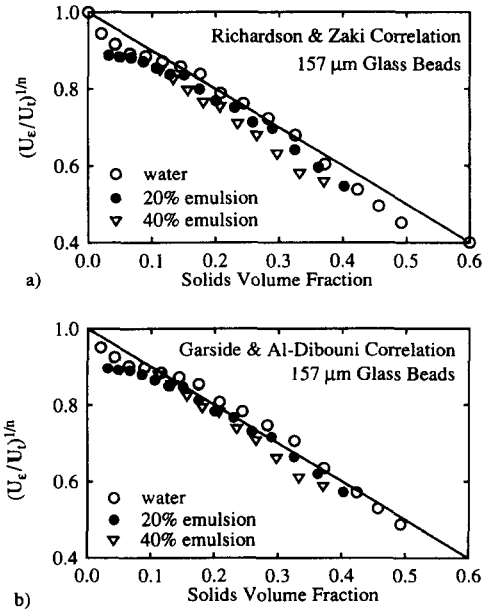


Figure 11. Solids settling data in water and in emulsions for the 157 μm glass beads.

Table 3. Relative velocity models

**Masliyah (1979) model:**

$$v_{\varepsilon,i,b} = \frac{u_{\varepsilon,i,m}}{\varepsilon^2}\frac{(\rho_i - \rho_b)}{(\rho_i - \rho_f)}, \quad i = l, h,$$

where

$$\rho_b = \rho_l \varphi_l + \rho_h \varphi_h + \rho_f \varepsilon.$$

**Mirza & Richardson (1979) model:**

$$v_{\varepsilon,i,b} = \frac{u_{\varepsilon,i,m}}{\varepsilon^{0.6}}, \quad i = l, h.$$

**Selim *et al.* (1983) model:**

$$v_{\varepsilon,i,b} = \frac{u_{\varepsilon,i,m}}{\varepsilon}\frac{(\rho_i - \rho_{m,i})}{(\rho_i - \rho_f)}, \quad i = l, h,$$

where

$$\rho_{m,i} = \frac{(\varepsilon\rho_f + \varphi_i\rho_i)}{(\varepsilon + \varphi_i)}, \quad i = l, h.$$

emulsions can be considered to behave as a continuum towards the solids. Moreover, both Richardson & Zaki's (1954) and Garside & Al-Dibouni's (1977) correlations agree well with the experimental velocity $U_\varepsilon/U_t$.

It was mentioned in the introduction that several models were proposed for predicting the settling velocity of dilute bidisperse systems (without fingering). Here we apply three relative velocity models to our 20% emulsion system where fingering was absent. Table 3 gives a listing of the relative velocity models. Both the oil droplets and the solids constitute the dispersed phase. The settling velocity of the heavy particles is related to the relative velocities by

$$U_\varepsilon = v_{\varepsilon,h,b}(1 - \phi_h) - v_{\varepsilon,l,b}\phi_l, \qquad [9]$$

where $\phi_h$ and $\phi_l$ are the volume fractions of the heavy and light species and $v_{\varepsilon,h,b}$ and $v_{\varepsilon,l,b}$ are the relative velocities of the heavy and light particles in a bidisperse phase. In table 3, $u_{\varepsilon,h,m}$ and $u_{\varepsilon,l,m}$ refer to the settling velocities of the heavy and light particles in their respective monodisperse systems.

For the 57 $\mu$m size solid, figure 12 shows the calculated velocity ratio $U_\varepsilon/U_t$ using [9] and the experimentally determined values. As can be seen, the three modles give divergent predictions and none of the models predict the settling rate accurately.

Comparison between figures 10 and 12 reveals that a better prediction of the settling velocity can be obtained by treating the emulsion as a continuum rather than treating the oil droplets as a distinct phase. Similar conclusions can be made for the 157 $\mu$m size solids.

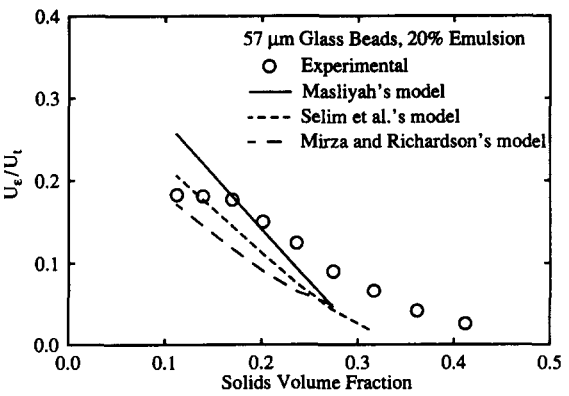


Figure 12. Prediction of the solids settling velocity using bidisperse models. Comparison with experimental data: 57 $\mu$m solids size and 20% emulsion.

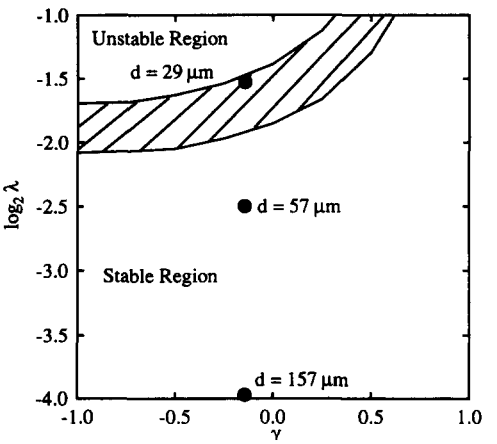


Figure 13. Prediction of the instability using Batchelor & Janse van Rensburg's (1986) experimentally constructed map.

*Analysis for the fingering phenomenon*

We now attempt to compare our experimental observations with those of Batchelor & Janse van Rensburg (1986) and use their instability theory to predict the structure formation for the different solids. It is to be noted, once again, that the stable and regular streams as observed in the present study and those reported by Fessas & Weiland (1984) did not seem to have occurred in Batchelor & Janse van Rensburg's (1986) experiments. It is also worth pointing out that the time scale for the establishment and duration of stable fingering streams is much longer than the irregular large-scale structures observed by Batchelor & Janse van Rensburg (1986). It may be true that in the latter case the inertia of the heavy particles is so much greater than that of the light ones that the disturbance created in the fluid prevents organized long streams from forming. Thus, it may be concluded that in the case of stable regular streams, the phenomenon is *viscous dominant*, whereas in the case of large random structures, the phenomenon is *inertia dominant*.

Based on their extensive *experimental* study for bidisperse suspensions for various size and density ratios, Batchelor & Janse van Rensburg were able to construct a map for the boundaries of stable and unstable regions. The bottom portion of the map is shown in figure 13. The map was constructed for a specific condition, where the volume fraction of both species was 0.15. The density ratio and the size ratio were defined as

$$\gamma = \frac{\rho_2 - \rho_0}{\rho_1 - \rho_0} \qquad [10]$$

and

$$\lambda = \frac{a_2}{a_1}, \qquad [11]$$

where $\rho$ represents the density and $a$ represents the diameter of solids. Subscripts 1 and 2 refer to species 1 and species 2, respectively, and 0 refers to the continuous fluid.

Their *experimental* results indicated that above the cross-hatched band, the bidisperse suspensions were unstable; and below the band, stable. The three sizes of glass beads ($\rho_1 = 2530\ \text{kg/m}^3$, $a_1 = 29, 57.157\ \mu\text{m}$) and the oil droplets ($\rho_2 = 780\ \text{kg/m}^3$, $a_2 \approx 10\ \mu\text{m}$) of the present study correspond to a density ratio of $\gamma = -0.143$ and size ratios of $\lambda = 0.347$, 0.177 and 0.0638. These three points are also shown in figure 13. For the 20% oil emulsions, at a solids volume fraction of 0.15, the oil volume fraction based on the total volume is $0.2\ (1 - 0.15) = 0.17$, which is close to the condition under which the map was constructed. As can be seen, for the small solids (29 $\mu$m), though the point lies within the band (marginally unstable), it is very close to the unstable region. Due to the experimental uncertainty in establishing the map, this point could well be above the band in the unstable region. Experimentally, strong fingering was observed for the small size solids settling in a 20% oil emulsion. For the 57 $\mu$m glass beads, at $\varphi_1 = \varphi_2 = 0.15$, the point falls below the cross-hatched band and is located in the stable region. This explains the fact that even at a solids volume fraction of 0.3 in a 20% emulsion, fingering was essentially not observed. Though at a higher oil concentration (40%) fingering was observed, the conditions corresponding to this high oil concentration are far too different from $\varphi_1 = \varphi_2 = 0.15$, under which the map was intended to apply. As for the large solids (157 $\mu$m), the data point falls well below the band. Thus, no instability should occur, as was indeed observed in our experiments.

Batchelor & Janse van Rensburg (1986) also established the following theoretical relation for predicting the onset of instability:

$$I = \left(\frac{\partial \varphi_1 U_1}{\partial \varphi_1} - \frac{\partial \varphi_2 U_2}{\partial \varphi_2}\right)^2 + 4\varphi_1 \varphi_2 \frac{\partial U_1}{\partial \varphi_2}\frac{\partial U_2}{\partial \varphi_1} < 0. \qquad [12]$$

We now try to apply this relation to our present system. For dilute suspensions, following Batchelor & Janse van Rensburg, we assume

$$U_1 \approx U_{10}(1 + S_{11}\varphi_1 + S_{12}\varphi_2) \qquad [13]$$

and

$$U_2 \approx U_{20}(1 + S_{21}\varphi_1 + S_{22}\varphi_2), \qquad [14]$$

Table 4. Sedimentation coefficients and $I$ values

| $a_1$ ($\mu$m) | $\gamma$ | $\lambda$ | $S_{11}, S_{22}$ | $S_{12}$ | $S_{21}$ | $I(\varphi_1 = \varphi_2 = 0.15)$ |
|---|---|---|---|---|---|---|
| 29 | −0.144 | 0.347 | −5.5 | −2.46 | 66.5 | $0.991U_{10}^2$ |
| 57 | −0.144 | 0.177 | −5.5 | −2.356 | 346.6 | $0.92U_{10}^2$ |
| 157 | −0.144 | 0.0638 | −5.5 | −2.356 | 2055 | $0.93U_{10}^2$ |

where $U_{10}$ and $U_{20}$ are the velocities of isolated paraticles of type 1 and 2, respectively. $S_{11}$, $S_{22}$, $S_{12}$ and $S_{21}$ are the sedimentation coefficients due to hydrodynamic interaction; $S_{11}$ and $S_{22}$ are for monodisperse systems, and $S_{12}$ and $S_{21}$ are for bidisperse systems due to hydrodynamic coupling of the two species. The numerical values and the asymptotic formulae for the sedimentation coefficients were provided by Batchelor & Wen (1982).

Carrying out all the necessary differentiations and noting that $U_{20} = \gamma\lambda^2 U_{10}$, we have the following expression:

$$I = U_{10}^2[1 + 2S_{11}\varphi_1 + S_{12}\varphi_2 - \lambda^2\gamma(1 + 2S_{22}\varphi_2 + S_{21}\varphi_1)]^2 + 4\varphi_1\varphi_2 U_{10}^2 S_{12} S_{21}\lambda^2\gamma. \quad [15]$$

Corresponding to the three sizes of the glass beads ($\gamma = -0.144$, $\lambda = 0.347$, 0.177 and 0.0638), the numerical values of the sedimentation coefficients as determined from Batchelor & Wen (1982) for the present system are listed in table 4.

For a dilute system, let us assume $\varphi_1 = \varphi_2 = 0.15$, which approximately corresponds to our 20% emulsion system, the numerical values of $I$ can be calculated and they are listed in table 4. As can be seen, all the values of $I$ are positive. However, as $U_{10}$ is proportional to $a_1^2$, the numerical values of $I$ should increase with $a_1^4$. Although the theory does not predict any fingering for any size solids, it does indicate a trend that as the solids size increases, the numerical value of $I$ increases in the manner of $a_1^4$. In other words, the possibility of fingering decreases with increasing solids size.

We also note from table 1 of Batchelor & Wen (1982) that for small values of $\gamma(|\gamma| \to 0)$, when $\lambda < 1$, all the values of $S_{12}$ are negative. Corresponding to these values of $\gamma$ and $\lambda$, $S_{21}$ is always positive for $\gamma < 0$ (note that while evaluating $S_{21}$, the reciprocals of $\gamma$ and $\lambda$ should be used). Thus, the term outside the brackets in [15] is always positive. This eliminates the possibility of finding any instability. Therefore, the theoretical analysis of Bachelor & Janse van Rensburg (1986) indicates that no fingering (instability) should occur for any size of solids at $\gamma = -0.144$ for the present system. While figure 13 clearly shows the possibility of fingering for certain sizes of solids at $\gamma = -0.144$, we do not note any apparent reason for this discrepancy between their theory and the map (experimentally determined) when applied to the present system.

## CONCLUSIONS

The fingering phenomenon (in the form of stable and regular vertical streams) was observed for the small solids settling in a 20% oil emulsion at solids volume fractions above 0.1. For the intermediate solids size, fingering did not occur when the solids were settling in a 20% oil emulsion, but fingering streams were formed in the case of a more concentrated emulsion (40%). No fingering occurred for the large solids at any solids volume fractions and at any oil concentrations as used in this study.

When fingering occurred for the case of small size solids, the apparent solids settling velocity and the emulsion creaming velocity were both increased significantly. When no stable streams were formed, the settling velocity can be better predicted by assuming the emulsions to form a continuous phase.

*Acknowledgements*—This work was financially supported by the Alberta Oil Sands Technology and Research Authority and by the Natural Science and Engineering Research Council of Canada.

## REFERENCES

BARNEA, E. & MIZRAHI, J. 1973 A generalized approach to the fluid dynamics of particular systems Part 1. General correlation of fluidization and sedimentation in solid multiparticle systems. *Chem. Engng J.* **5**, 171–189.

BATCHELOR, G. K. & JANSE VAN RENSBURG, R. W. 1986 Structure formation in bidisperse sedimentation. *J. Fluid Mech.* **166,** 379–407.

BATCHELOR, G. K. & WEN, C.-S. 1982 Sedimentation in a dilute polydisperse system of interacting spheres. Part 2. Numerical results. *J. Fluid Mech.* **124,** 495–528.

CLIFT, R., GRACE, J. R. & WEBER, M. E. 1978 *Bubbles, Drops and Particles.* Academic Press, New York.

FESSAS, Y. P. & WEILAND, R. H. 1981 Convective solids settling induced by a buoyant phase. *AIChE Jl* **27,** 588–592.

FESSAS, Y. P. & WEILAND, R. H. 1982 Convective solids settling induced by a buoyant phase—a new method for acceleration of thickening. *Resour. Conserv.* **9,** 87–93.

FESSAS, Y. P. & WEILAND, R. H. 1984 The settling of suspension promoted by rigid buoyant particles. *Int. J. Multiphase Flow* **10,** 485–507.

FRANCIS, A. W. 1933 Wall effect in falling ball method for viscosity. *Physics* **4,** 403–406.

GARSIDE, J. & AL-DIBOUNI, M. R. 1977 Velocity–voidage relationship for fluidization and sedimentation in solids–liquid systems. *Ind. Engng Chem Proc. Des. Dev.* **16,** 206–214.

LAW, H.-S., MASLIYAH, J. H., MACTAGGART, R. & NANDAKUMAR, K. 1987 Gravity separation of bidisperse suspensions: light and heavy particle species. *Chem. Engng Sci.* **42,** 1527–1538.

LOCKETT, M. J. & AL-HABBOOBY, H. M. 1974 Relative particle velocities in two species settling. *Power Technol.* **10,** 67–71.

MACTAGGART, R. S., LAW, H.-S. D., MASLIYAH, J. H. & NANDAKUMAR, K. 1988 Gravity separation of concentrated bidisperse suspensions in inclined plate settlers. *Int. J. Multiphase Flow* **14,** 519–532.

MASLIYAH, J. H. 1979 Hindered settling in a multi-species particle system. *Chem. Engng Sci.* **34,** 1166–1168.

MIRZA, S. & RICHARDSON, J. F. 1979 Sedimentation of suspension of particles of two or more sizes. *Chem. Engng Sci.* **34,** 447–454.

PATWARDHAN, V. S. & TIEN, C. 1985 Sedimentation and liquid fluidization of solids particles of different sizes and densities. *Chem. Engng Sci.* **40,** 1051–1060.

RICHARDSON, J. F. & ZAKI, W N. 1954 Sedimentation and fluidization: Part 1. *Trans. Instn Chem. Engrs* **32,** 35–53.

SELIM, M. S, KOTHARI, A. C. & TURIAN, R. M. 1983 Sedimentation of multi-sized particles in concentrated suspensions. *AIChE Jl* **29,** 1029–1038.

WEILAND, R. H. & MCPHERSON, R. R. 1979 Accelerated settling by addition of buoyant particles. *Ind. Engng Chem. Fundam.* **18,** 45–49.

WEILAND, R. H., FESSAS, Y. P. & RAMARAO, B. V. 1984 On instabilities arising during sedimentation of two-component mixtures of solids. *J. Fluid Mech.* **142,** 383–389.

WHITMORE, R. L. 1955 The sedimentation of suspensions of spheres. *Br. J. Appl. Phys.* **6,** 239–245.

YAN, Y. & MASLIYAH, J. H. 1993 Effect of oil viscosity on the rheology of oil-in-water emulsions with added solids. *Can. J. Chem. Engng.* In press.

YAN, Y., PAL, R. & MASLIYAH, J. H. 1991 Rheology of oil-in-water emulsions with added solids. *Chem. Engng Sci.* **46,** 985–994.